Supplementary Materials

1. Determination of the Angle of Incidence and Thin Layer Cavity Thickness

In this section, *R(e)* denotes the single beam reflectivity from the three phase system, Pt|H_2O|ZnSe, *R(a)* is the single beam reflectivity from the air|ZnSe interface and *R(s)* single beam reflectivity from the H_2O|ZnSe interface. The procedure used to determine the angle of incidence and the thin layer cavity thickness has been described in ref 32 and 38 of this paper. In short, the method first involves the measurement of the reflectivity for the empty IR cell, *R(a)*. Next the cell is filled with sulfate solution and the Pt electrode is inserted and pressed up against the IR window to form the thin layer configuration. The reflectivity for the electrode|solution|window interface, *R(e)*, is measured. The ratio *R(e)/R(a)* is calculated from the experimental data and Fresnel equations in the matrix form are used to calculate *R(e)/R(a)* from the optical constants of the electrode, solution and the window. The initial value of the angle of incidence is determined from the geometry of the optical set-up. However, the angle of incidence and thin layer cavity thickness are two adjustable parameters in the Fresnel matrix, which are used to fit the experimental data to produce a calculated curve of best fit. Therefore the final value of the angle of incidence may be different than the initial

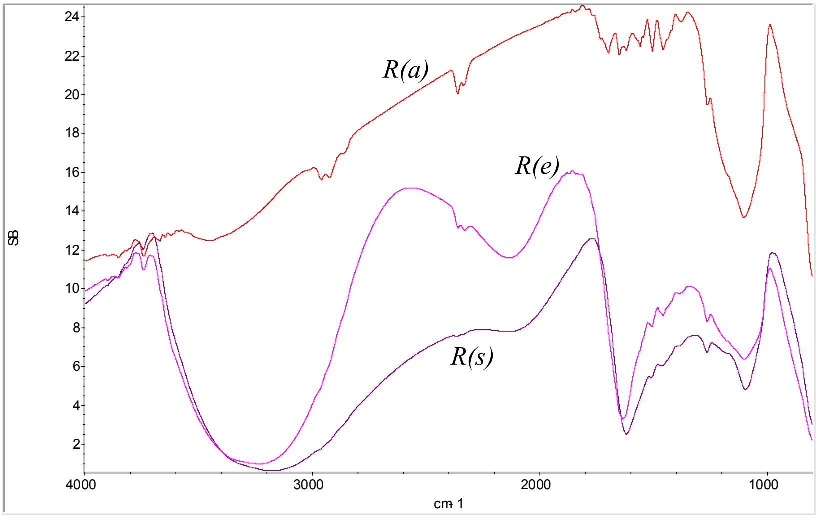

Fig. 1 Single beam reflectivities from: *R(e)* – Pt|H_2O|ZnSe; *R(a)* – air|ZnSe and *R(s)* – H_2O|ZnSe interface when the system was optimized to angle incidence ~31°.

estimate based on the geometry of the optical set-up.

In the present study, the optical set-up was aligned to carry out experiments at an angle of incidence ~31°, which according to recent calculations (ref.45 in this paper), is close to the global maximum of the mean squared electric field strength (MSEFS) for IR adsorption of sulfate. However, this particular angle of incidence is also close to the critical angle of the ZnSe|H_2O interface. Fig. 1 illustrates that a significant reflection of IR radiation occurs at the window|solution interface.

The single beam reflectivities of the three interfaces acquired from the experimental configuration optimized at an incidence angle of ~31° are plotted in Fig. 1. The data clearly shows that the values of *R(e)* and *R(s)* for the wavenumber range of approximately 1800 – 1600 cm^{-1} and those larger than 3100 cm^{-1} are identical. In these two regions, the reflectivity that is measured for the Pt|H_2O|ZnSe system is essentially determined by the reflectivity at the H_2O|ZnSe interface making the signal from the three-phase system negligible. Note: the reflectivity from the Pt|H_2O|ZnSe system cannot be less than the reflectivity from the H_2O|ZnSe interface.

The implication of this phenomenon is significant in the calculation of the angle of incidence and thin cavity thickness. Fig. 2 shows a typical "good" fit to the *R(e)/R(a)* data. The fit was performed in the range ~3500 – 1400 cm^{-1}. However, as shown from the single reflectivities in Fig. 1, the two deep minima in the experimental *R(e)/R(a)* curve of Fig. 2 are misleading since the reflectivity in these regions occur at the H_2O|ZnSe interface and not from the desired Pt|H_2O|ZnSe system.

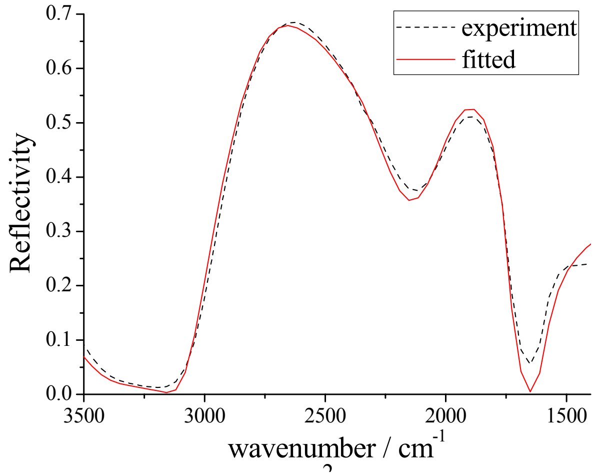

Fig. 2 Experimental (dashed line) and fitted IR reflectivity (dotted line) of the Pt(111) electrode in 0.1 M Na_2SO_4 + 0.001 M H_2SO_4 solution for p-polarized light. The fitted incident angle and water gap thickness are 28.5^0 and 5.0 μm

The fits for this data provide incorrect values for the thin layer thickness and unusually low angles of incidence of approximately 28^o. As a result, the MSEFS that is calculated using these values did not allow for correct subtraction of the IR contribution from the solution species in the p-polarized SNIFTIR spectra since the s-polarized IR spectra must be multiplied by the ratio of the MSEFS for p- and s-polarized radiation as shown in the following equation: $\left(\frac{\Delta R}{R}\right)_s \times \frac{<E_{p,ave,0\rightarrow gap}>^2}{<E_{s,ave,0\rightarrow gap}>^2}$. This point is illustrated in Fig. 3, which shows that the resulting s-polarized spectrum after correcting for the calculated field strength (shown in black) has a positive band at ~1100 cm^{-1}. The intensity of this band is approximately ½ of that observed in the spectrum acquired using p-polarized light (shown in red). After subtraction of the corrected spectrum for s-polarization from the spectrum for p-polarization the features due to the solution species are not removed (shown in blue).

However, despite this complication, the single reflectivities in Figure 1 can still be used to calculate *R(s)/R(a)* and these curves could be used to calculate correct thin

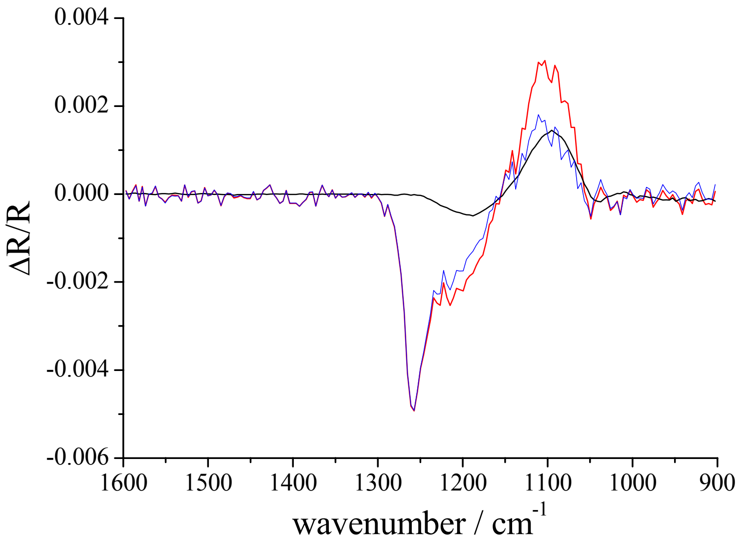

Fig.3 Calculated IR spectra of the Pt(111) electrode in 0.1 M Na_2SO_4 + 0.001 M H_2SO_4 solution as: $(\frac{\Delta R}{R})_p$ (red), $(\frac{\Delta R}{R})_s \times \frac{<E_{p,ave}>^2}{<E_{s,ave}>^2}$ (black), and $(\frac{\Delta R}{R})_p - \left(\frac{\Delta R}{R}\right)_s \times \frac{<E_{p,ave}>^2}{<E_{s,ave}>^2}$ (blue). The incident angle and cavity thickness is 28.5^o, 5.0 μm.

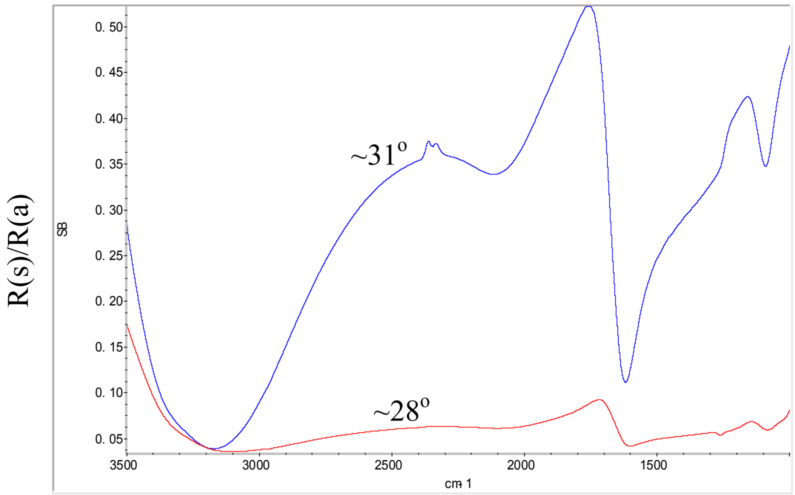

Fig. 4 Ratio of reflectivities from the window|solution to the window|air interface for two configurations of the experimental system optimized for the angle of incidence ~31° and ~28° (p-polarized light).

layer thickness and angle of incidence. Fig. 4 plots the experimental *R(s)/R(a)* curves for two configurations of the experimental set-up; optimized for ~31° (top curve) and optimized for ~28° bottom curve. Fig. 5 plots the simulated *R(s)/R(a)* curves for several angles of incidence. The simulated curves reproduce the experimental. It can be seen that the reflectivity of ZnSe|H_2O interface is increasing with the increase in the angle of incidence.

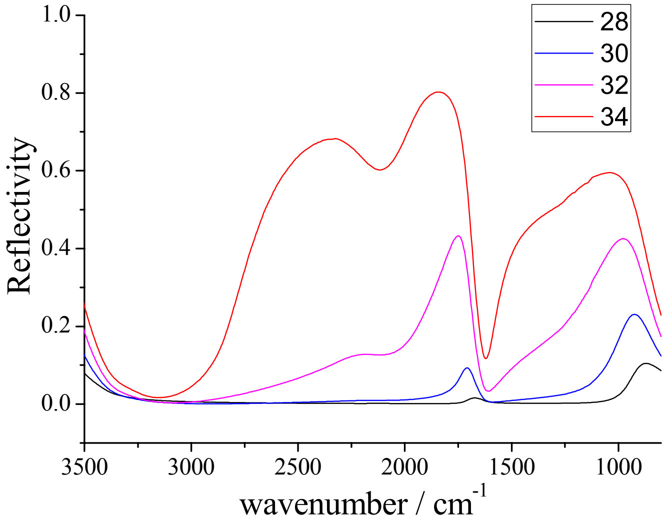

Fig. 5 For ZnSe|H_2O system, simulated R(s)/R(a) curves for various angles of incidence, p-polarized light.

At this point, the data treatment procedure was altered. The angle of incidence was determined from the *R(s)/R(a)* curve and then the thickness of the thin layer cavity was determined from the fit of *R(e)/R(a)* in the range between 3000 – 1800 cm^{-1} wavenumbers where *R(e)>R(s)*. The angle of incidence was only allowed to vary only $\pm 1^{\circ}$ from the value determined from the *R(s)/R(a)* curve. The fit shown in Fig. 6 A was performed using formula $R = \dfrac{f^* R(e) - R(s)}{R(a) - R(s)}$. The fit in Fig. 6B was performed using the formula $R = \dfrac{f^* R(e) - R(s)}{R(a)}$ where $f^* \sim 1.1$ is a factor taking into account that the electrode size was smaller than the footprint of the IR beam.

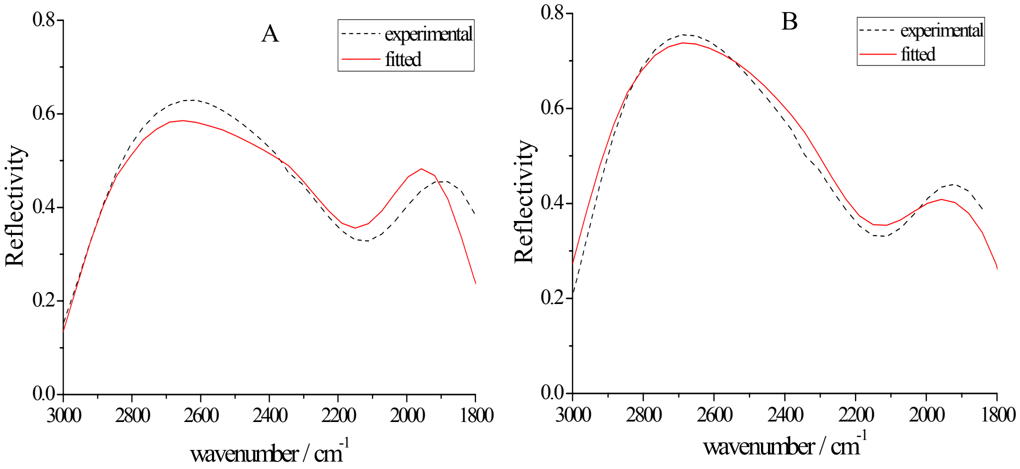

Fig. 6 Experimental and fitted IR reflectivity of the Pt(111) electrode in 0.1 M Na_2SO_4 + 0.001 M H_2SO_4 solution for p-polarized light. A: The fitted angle of incidence and cavity thickness are 31^0 and 4.9 μm. B: The fitted angle of incidence and the cavity thickness are 31^0 and 2.8 μm.

With these new values for the angle of incidence and cavity thickness, the s-polarized spectrum, after correcting for the ratio of the MSEFS, can be used to properly remove the IR contributions from solution species in the p-polarized spectrum, which is illustrated in Fig. 7.

Fig. 7A and 7B show the correction of the p-polarized spectra using the angles of incidence and the cavity thicknesses determined from the fitted curves in Fig. 6A and 6B, respectively. It appears that the experimental spectrum in Fig. 7A, fit using the data from Fig. 6A, gives a somewhat better correction compared to the p-polarized spectrum in Fig. 7B, which was fit with the parameters obtained from Fig. 6B.

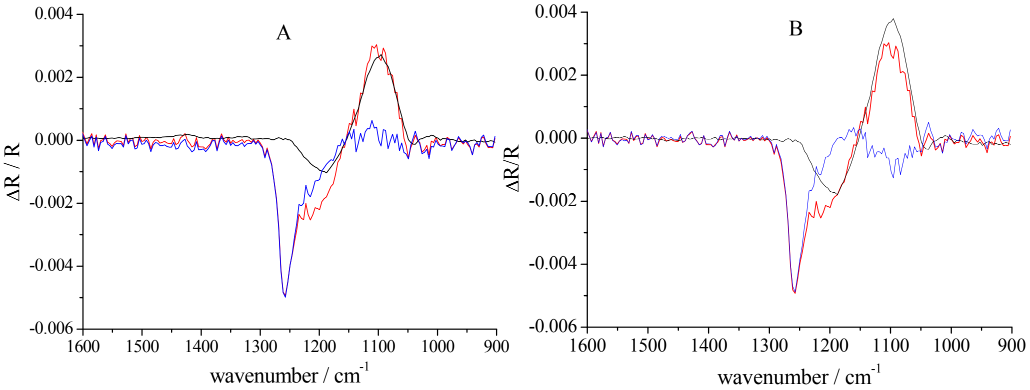

Fig. 7 Calculated IR spectra of the Pt(111) electrode in 0.1 M Na_2SO_4 + 0.001 M H_2SO_4 solution in terms of $\left(\frac{\Delta R}{R}\right)_p$ (red), $\left(\frac{\Delta R}{R}\right)_s \times \frac{<E_{p,ave}>^2}{<E_{s,ave}>^2}$ (black) and $\left(\frac{\Delta R}{R}\right)_p - \left(\frac{\Delta R}{R}\right)_s \times \frac{<E_{p,ave}>^2}{<E_{s,ave}>^2}$ (blue).

To check this procedure, the optical system was realigned to an angle of incidence ~28°. Fig. 8 plots the corresponding single reflectivities at this new alignment. The reflectivity at the H_2O|ZnSe interface is now much smaller than the reflectivity at the Au|H_2O|ZnSe spectrum in the wavenumber range of 1200 – 3000 cm^{-1}.

This spectral range is used to calculate the thin cavity thickness and angle incidence from the ratio *R(e)/R(a)* using standard procedure described in references 32 and 38. The Fig. 9A shows that the fit from this procedure is quite poor. The Fig. 9B shows a superior good fit to the experimental data using {*R(e)-R(s)*}/*R(a)* where the

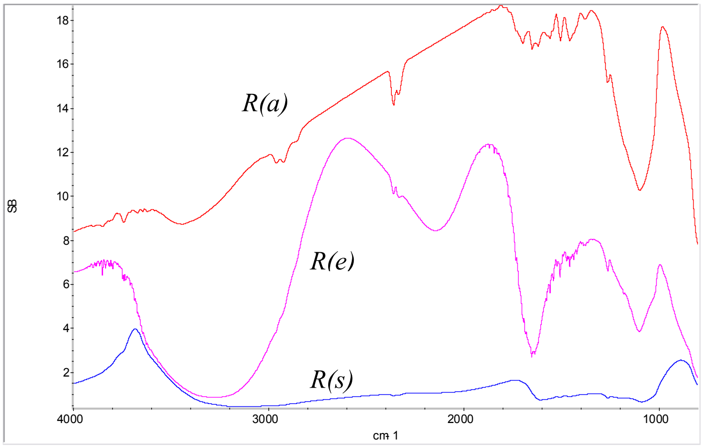

Fig. 8 Single beam reflectivities obtained from: *R(e)* – Pt|H_2O|ZnSe; *R(a)* – air|ZnSe and *R(s)* – H_2O|ZnSe interface when the system was optimized to angle incidence ~28° in a 0.1 M Na_2SO_4 + 0.001 M H_2SO_4 solution.

reflectivity *R(e)* was corrected for the reflectivity at the window|solution interface. The angle and thickness parameters determined from the fit are 28^o and 4.1 μm, respectively.

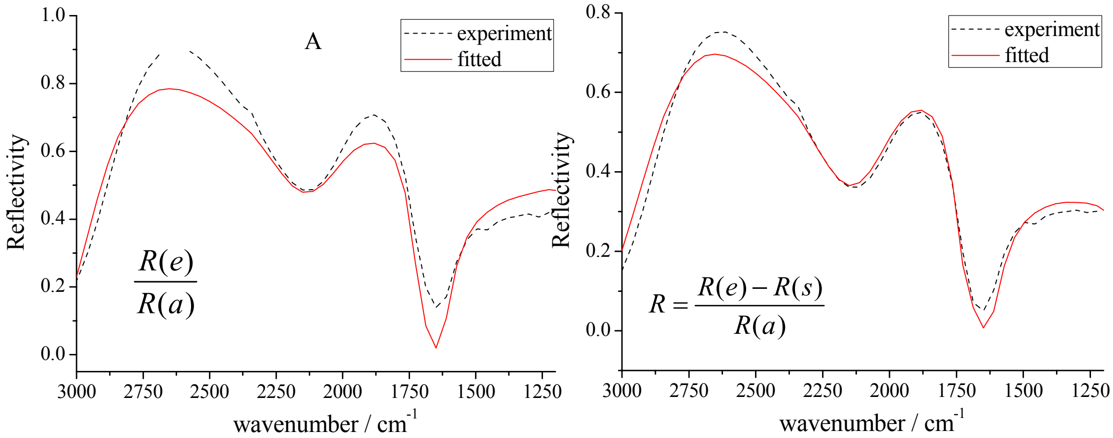

Fig. 9 Fits of the thin cavity thickness for the Pt(111) electrode in 0.1 M Na_2SO_4 + 0.001 M H_2SO_4 solution with the setup aligned for ~28^o angle of incidence. Left panel shows the fit for R(e)/R(a) and right panel is the fit for {R(e)-R(s)}/R(a). The angle of incidence and thin cavity thickness for the right panel is 28^0 and 4.1 μm, respectively.

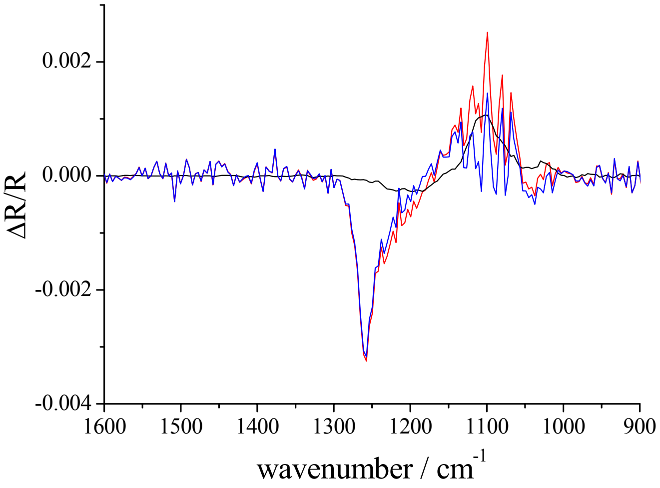

Fig. 10 Calculated IR spectra of the Pt(111) electrode in 0.1 M Na_2SO_4 + 0.001 M H_2SO_4 solution as: $\left(\frac{\Delta R}{R}\right)_p$ (red), $\left(\frac{\Delta R}{R}\right)_s \times \frac{< E_{p,ave} >^2}{< E_{s,ave} >^2}$ (black), and (c): $\left(\frac{\Delta R}{R}\right)_p - \left(\frac{\Delta R}{R}\right)_s \times \frac{< E_{p,ave} >^2}{< E_{s,ave} >^2}$ (blue) for the experiment where the incident angle and cavity thickness is 28^0 and 4.1μm, respectively.

Using these values for the angle of incidence and cavity thickness, the spectra acquired using s-polarized light multiplied by the ratio of MSEFS shows a good fit with features observed by the species in solution for p-polarized spectrum, which is illustrated in Fig. 10 (Note: the S/N for the spectra in Fig. 10 is much poorer than the spectra shown in Fig. 7 since the surface enhancement at ~28^o is less than that at ~31^o).

Finally, ΔR_{ads} can be calculated for two experiments at 28^o and 31^o angle of incidence using the following expression:

$$\Delta R_{ads} = \frac{\left(\frac{\Delta R}{R}\right)_p - \left(\frac{\Delta R}{R}\right)_s \times \frac{< E_{p,average} >^2}{< E_{s,average} >^2}}{< E_{p,z=0} >^2}$$

The resulting calculated spectra are shown in Fig. 11 where ΔR_{ads} should be independent of gap thickness and incident angle. It can be seen the shape and intensity of ΔR_{ads} is very similar in two experiments, confirming the accuracy of our procedure.

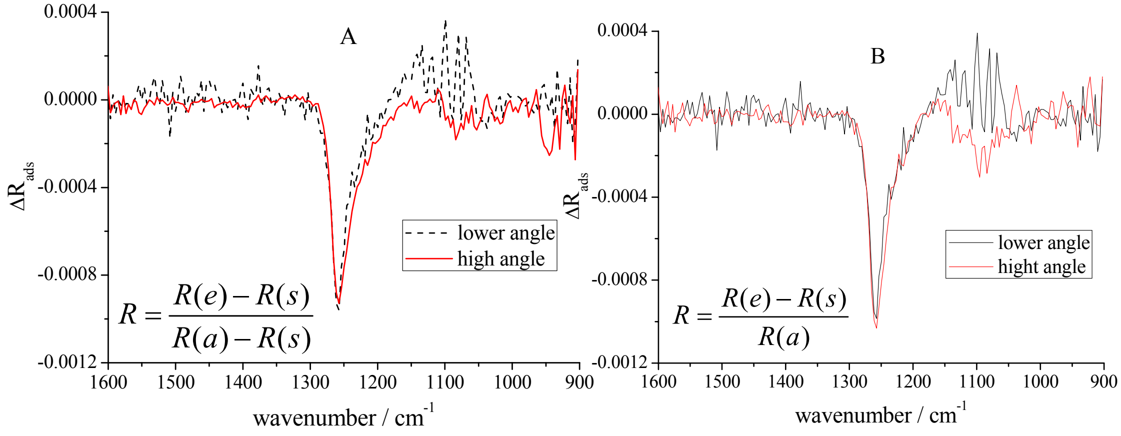

Fig. 11 ΔR_{ads} spectra calculated for the two experiments; red line 31^o and black line 28^o angle of incidence. The reflectivity of electrode surface is calculated by different formulas.

Conclusions

1. When working with a ZnSe prism at an incident angle near of the global maximum of the MSEFS, one cannot use the standard method of fitting the experimental *R(e)/R(a)* data to the ratio calculated from optical constants since the reflectivity at the H_2O|ZnSe is too high. In the regions that correspond to strong water absorption (above 3000 cm^{-1} and ~1650 cm^{-1}), the IR radiation is primarily reflected from the window|water interface and the shape of the water bands is distorted in experimental *R(e)/R(a)* spectrum.

2. The calculated fit to {*R(e)-R(s)*}/{*R(a)-R(s)*} always results in a better fit than

R(e)/R(a) since the reflectivities *R(e)* and *R(a)* are corrected for the IR reflectivity at the window|solution interface.

3. In future experiments, the single reflectivities of *R(e)*, *R(s)* and *R(a)* should be compared prior to performing any SNIFTIRS experiment in order to decide on the most appropriate method for determining the correct angle of incidence and thin layer cavity thickness.

2. CV curves of the Pt(111) electrode 0.001 M H_2SO_4 + 0.1 M Na_2SO_4 solution before and after IR experiment

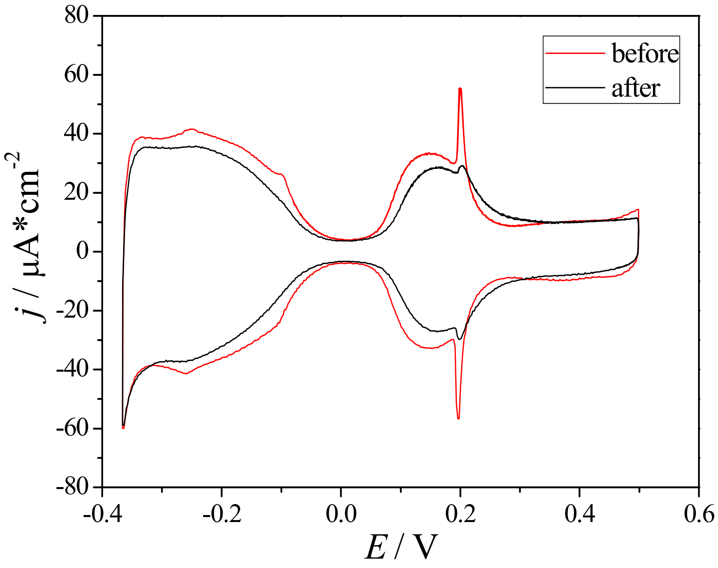

Fig. 12 CV curves of the Pt(111) electrode 0.001 M H_2SO_4 + 0.1 M Na_2SO_4 solution before and after IR experiment. The scan rate is 50 mV•s^{-1}

3. SNIFTIR Spectra of the Pt(111) Electrode in 0.1 M Na_2SO_4 + 0.001 M H_2SO_4 Solution at Different E_S

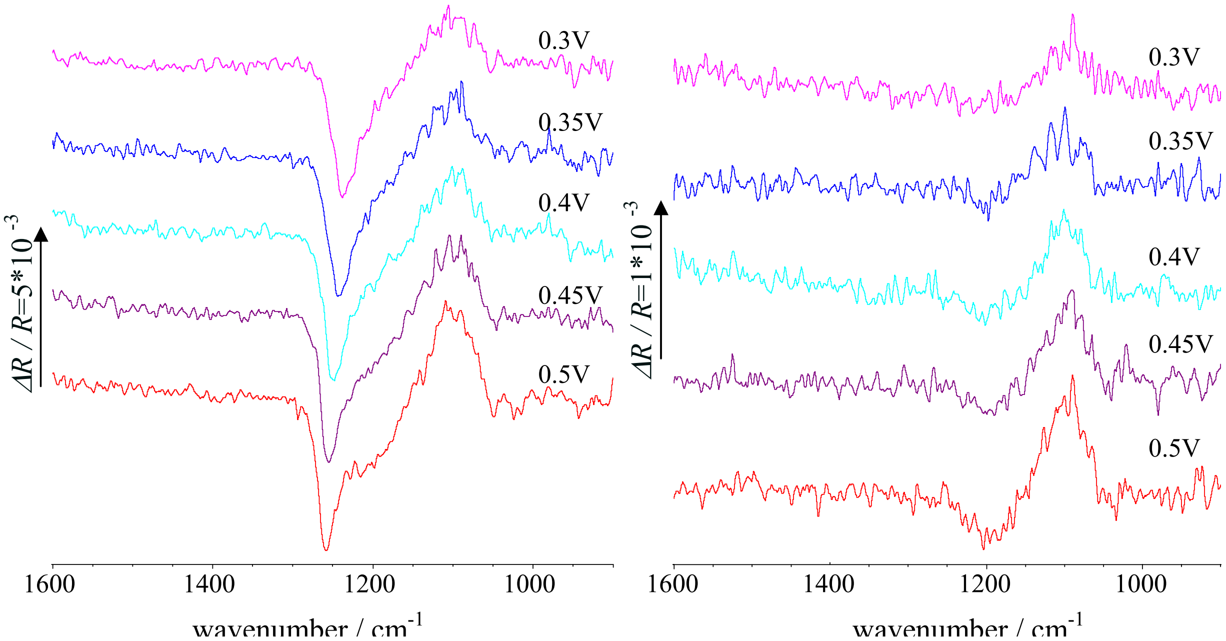

A

B

Fig. 13 SNIFTIRS spectra of the Pt(111) electrode in 0.1 M Na_2SO_4 + 0.001 M H_2SO_4 solution at (A) p-polarized light, and (B) s-polarized light. E_S is indicated in the figure, and E_R is 0.04 V.

4. ΔR_{ads} Spectra of the Pt(111) Electrode in 0.1 M Na_2SO_4 + 0.001 M H_2SO_4 Solution at Different E_S

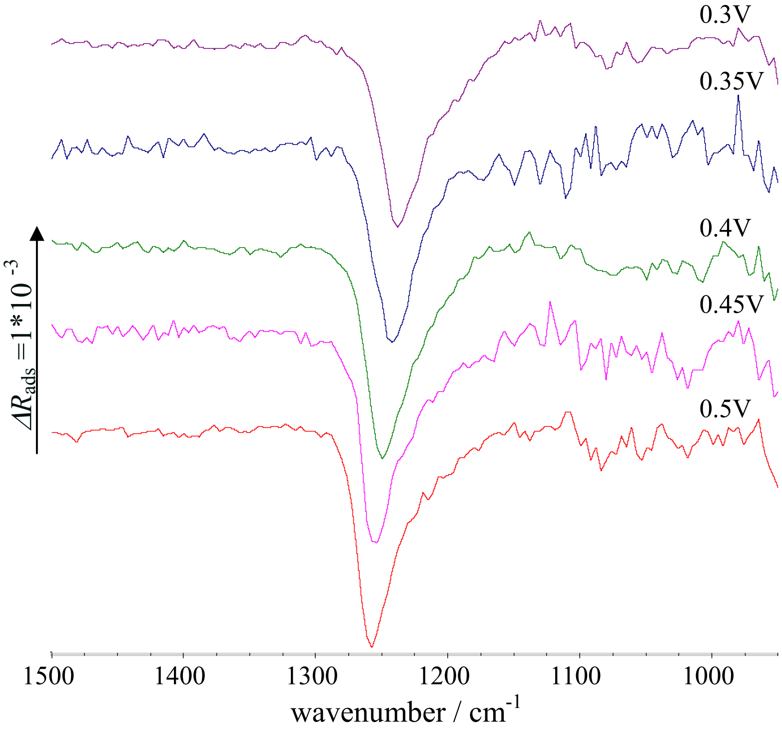

Fig. 14 ΔR_{ads} spectra of the Pt(111) electrode in 0.1 M Na_2SO_4 + 0.001 M H_2SO_4 solution. E_S is indicated in the figure.